# Disentangling drought-responsive traits with focus on Arabidopsis

Thonglim, A.

**Citation**

Thonglim, A. (2023, November 9). *Disentangling drought-responsive traits with focus on Arabidopsis*. Retrieved from https://hdl.handle.net/1887/3656528

## Chapter 1

# GENERAL INTRODUCTION AND THESIS OUTLINE

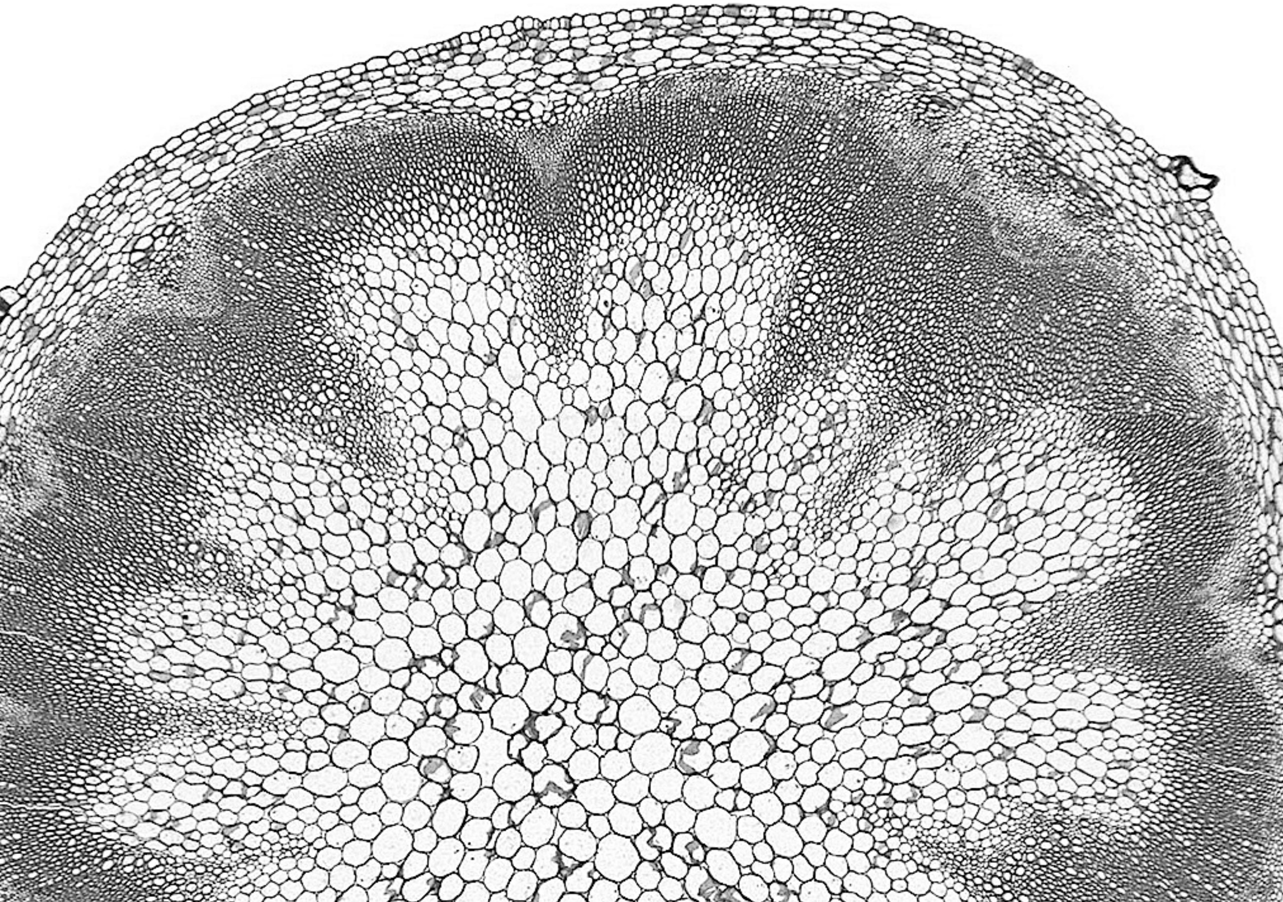

## *Impact of global warming on forest mortality and crop yield*

Temperature and precipitation patterns are shifting globally due to ongoing global warming. As a result, we are witnessing an increase in the severity and frequency of drought periods, even in countries that have not previously suffered drought stress (Corso *et al.*, 2020; Gleason *et al.*, 2022). These droughts have caused large-scale mortality events in various types of forests and ecosystems (Allen *et al.*, 2009, 2015; Hartmann *et al.*, 2018; Hammond *et al.*, 2022), such as temperate deciduous and evergreen forests (Crouchet *et al.*, 2019; Schuldt *et al.*, 2020), semi-arid woodlands and savannahs (Swemmer, 2020; Kannenberg *et al.*, 2021), dry tropical forests (Powers *et al.*, 2020), and tropical rainforests (Feldpausch *et al.*, 2016; Esquivel-Muelbert *et al.*, 2020) (Figure 1). Extensive and severe drought periods are also causing significant reductions in crop yield globally, with about 75% of the global harvested area experiencing drought-related yield losses (IPCC, 2022). Climate change has significantly impacted yields of nearly all important crops in Europe, particularly in southern Europe, resulting in recent yield stagnation and crop losses that have tripled over the past 50 years (Agnolucci and De Lipsis, 2020; Brás *et al.*, 2021). In western Africa, the declining precipitation and rising temperatures decrease millet and sorghum yields by 10–20% and 5–15%, respectively (Sultan *et al.*, 2019). Moreover, the combined effects of increased temperature and drought diminish the global yields of wheat, maize, and soybean by 9.2%, 11.6%, and 12.4%, respectively (Matiu *et al.*, 2017). Both crop yield decline and forest mortality are predicted to drastically accelerate at a global scale in the near future (Allen *et al.*, 2009; Lesk *et al.*, 2016; Klein and Hartmann, 2018; Goulart *et al.*, 2021; McDowell *et al.*, 2022). Moreover, drought stress frequently interacts with wildfires, windthrow (Brando *et al.*, 2014), or insect attacks (Temperli *et al.*, 2013; Sangüesa-Barreda *et al.*, 2015; Kolb *et al.*, 2016; Canelles *et al.*, 2021), which can exacerbate changes in the structure and function of natural ecosystems and agriculture (Waring *et al.*, 2009; Adams *et al.*, 2012; Clark *et al.*, 2016). Given the significant ecological and economic impacts of climate change, understanding drought-related plant death and its underlying mechanisms is crucial for accurately estimating the risk of forest and agricultural loss and implementing suitable management strategies (Anderegg *et al.*, 2013; Hartmann *et al.*, 2018).

The mechanisms underlying drought-induced mortality are complex. They involve the interplay between water, carbon, and biotic interdependencies (Anderegg *et al.*, 2015; McDowell *et al.*, 2022). The water and carbon supply are crucial for the survival of plants since they provide the basis for osmoregulation and cell maintenance (Koster and Leopold, 1988; Yu, 1999; Hoekstra *et al.*, 2001; Ramel *et al.*, 2009; Matros *et al.*, 2015; Martinez-Vilalta *et al.*, 2019; Mantova *et al.*, 2021; Sapes *et al.*, 2021), as well as the production of compounds used in a defense system against the attack of biotic agents (Goodsman *et al.*, 2013; Netherer *et al.*, 2015; Wiley *et al.*, 2016; Rissanen *et al.*, 2021). Furthermore, a decrease in carbon pool sizes and fluxes can impair resistance to embolism because carbohydrate is required to avoid, or tolerate cell dehydration, which is essential for maintaining the integrity of the hydraulic system (Tomasella *et al.*, 2019). Among all the processes involved in drought-induced plant mortality, carbon starvation and hydraulic failure have been proposed as the main mechanisms. Hydraulic failure occurs when the root-to-shoot water transport system collapses due to the accumulation of drought-induced embolism inside xylem conduits that exceeds the point at which water transport is irrecoverable (Sperry and Tyree, 1988; Venturas *et al.*, 2017; McDowell *et al.*, 2022; Johnson *et al.*, 2022). Carbon starvation occurs when the carbon-metabolic functions are impaired due to a limited supply of carbohydrates caused by a decrease in photosynthesis and available carbon storage (McDowell *et al.*, 2008, 2011). Although these two mechanisms are not mutually exclusive processes, many studies have shown that hydraulic failure is the primary cause of intense, short-to-longer periods of drought (Urli *et al.*, 2013; Salmon *et al.*, 2015; Adams *et al.*, 2017; Mantova *et al.*, 2022*b*), while carbon starvation is more likely to happen during prolonged moderate drought conditions (McDowell *et al.*, 2008; Creek *et al.*, 2020).

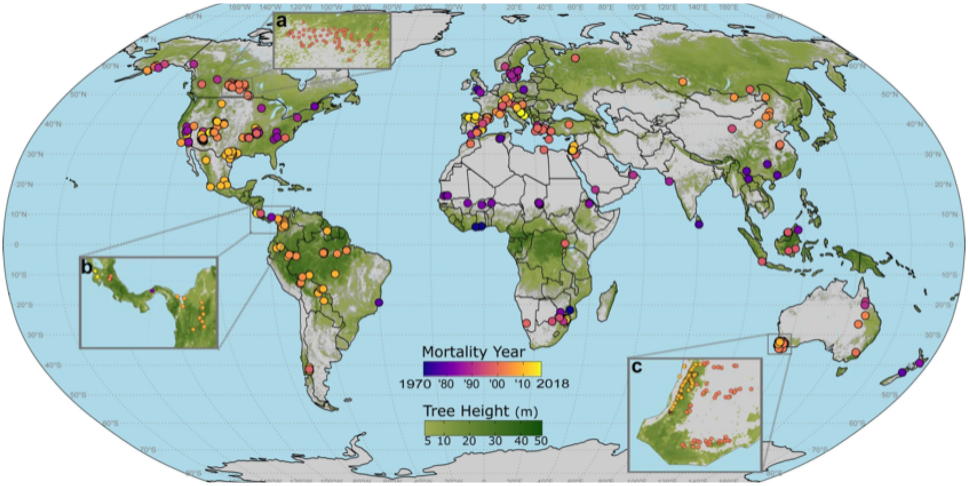

**Figure 1** A global map showing forest mortality locations associated with drought and high temperatures induced by climate change. Each dot represents a color-coded forest mortality event according to the year of mortality. *Taken from Hammond et al. (2022).*

## *Plant vascular tissue: development and growth*

To understand the mechanisms behind water transport in plants, it is important to first become familiar with the tissues involved in this process. The vascular tissue is a crucial component of plants, originating from meristem cells called procambium located in the plant axis (root and stem) during embryonic development and beyond. These procambium strands produce vascular bundles comprising (primary) xylem that is lignin-rich and phloem that usually lacks lignin in the cell walls (Esau, 1965; Evert, 2006). Xylem transports water and nutrients upwards, whereas phloem transports sugars and other organic compounds from leaves to all living cells (Evert, 2006; Lucas *et al.*, 2013). The development of vascular tissues in the stem can be divided into two main stages: primary growth and (if available) secondary growth. *Primary growth* gives rise to all primary tissues by apical meristems in stems and roots, as well as by the procambium strands that produce the vascular bundles, and typically leads to plant elongation (Figure 2, i). *Secondary growth* is the developmental process in woody species – i.e., trees, shrubs, and lianas – that increases stem and root thickness through the activity of two lateral (secondary) meristems, known as vascular cambium and cork cambium. During secondary growth, vascular cambium cells divide and differentiate into wood (i.e., secondary xylem) towards the inside and secondary phloem towards the outside of the hollow cylindric meristem that connects the (intrafascicular) vascular cambium parts among adjacent vascular bundles via the formation of interfascicular cambium (Figure 2, ii-iv). Wood formation accumulates much faster than secondary phloem, which enlarges the vascular cambium and subsequently triggers the formation of cork cambium that produces the periderm with many cork cells (Figure 2, iii-iv). These cork cells act as a secondary protective barrier that helps to prevent water loss, protects the woody plant from physical damage, provides insulation (Esau, 1965; Pereira, 2007), and replaces the initial (primary) protective layer – epidermis in stems and rhizodermis in roots – that will rupture during the initial stages of the lateral growth. As the woody plant ages, the secondary xylem accumulates, forming a wood cylinder that provides essential structural stability and supports to the stem, and becomes responsible for a large part of the root-to-shoot water transport (Esau, 1965; Lucas *et al.*, 2013). At the same time, the bark tissues outside the vascular cambium develop as well, including secondary phloem that remains active for a limited amount of time, cortex parenchyma that often has the ability to undergo cell divisions to avoid rupturing during dilation, and (one or multiple) periderm(s) that include a cork cambium generating radial rows of cork cells towards the outside and one cell layer of phelloderm towards the inside (Esau, 1965; Pereira, 2007). These primary and secondary growth processes continue throughout the plant's lifetime, resulting in the continuous addition of new (primary and secondary) xylem and phloem and cork tissue, and a corresponding increase in vertical and lateral growth (Esau, 1965; Evert, 2006; Lucas *et al.*, 2013; Lopez and Barclay, 2017).

Unlike woody plants, herbaceous species rarely undergo secondary growth, and their lignified xylem tissue is mainly formed by the primary xylem inside the vascular bundles (Figure 2, i). Nevertheless, many non-monocot herbaceous angiosperm species have some degree of wood formation, although this is typically limited to the base of their stems (Schweingruber, 2006, 2007; Schweingruber *et al.*, 2011; Lens *et al.*, 2012*a*). In some cases, the limited amount of wood formation is confined to the vascular bundle regions at the base of the stem, while in others, a complete vascular cambium may be formed, producing a small cylinder of wood (Altamura *et al.*, 2001; Chaffey *et al.*, 2002; Lens *et al.*, 2012*a*; Ragni and Greb, 2018) (Figure 2, ii-iii). Due to the negligible presence of secondary development in herbaceous plants, their stems are mechanically weaker than those of woody species. Subsequently, lignification in cells outside the xylem plays a vital role in increasing the tensile strength and stiffness of herbaceous stems, thereby reducing the risk of breakage or damage (Barros *et al.*, 2015) (Figure 2, iii). In addition, lignified cells provide a barrier against pathogens and pests, protecting plants from disease (Barros *et al.*, 2015; Liu *et al.*, 2018), and also occur in other cell types in different organs of the plant, such as seeds and fruits (Barcelo, 1997; Barros *et al.*, 2015; Emonet and Hay, 2022). In conclusion, lignification and wood formation are two distinct processes in plant development. Yet, they resemble each other in incorporating lignin inside the cell walls, either inside the secondary xylem tissue during wood formation or outside the xylem tissue (lignified sclerenchyma cells in stems, roots, leaves, and fruits).

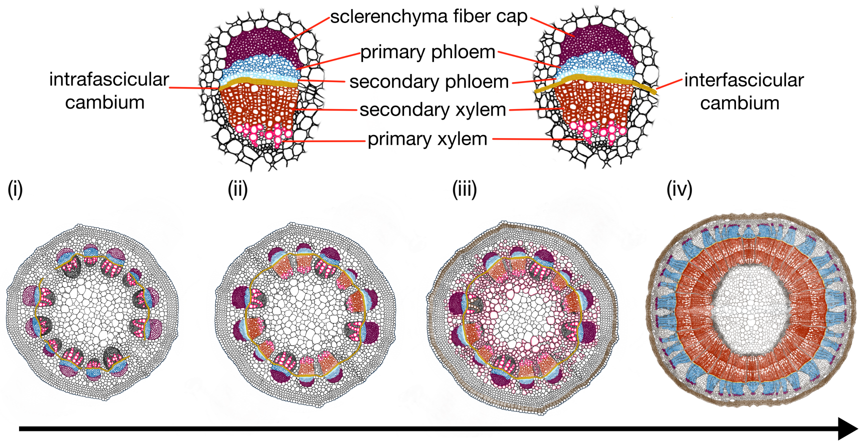

**Figure 2** A diagram illustrating the transition from primary to secondary growth in the stem (i to iv).

The process leads to an increase in the stem's thickness. It originates by connecting the intrafascicular cambium (within the vascular bundles) with interfascicular cambium parts (between the vascular bundles). At the beginning of secondary growth, the parenchyma cells close to the intrafascicular cambium dedifferentiate and undergo periclinal cell divisions, thereby forming a closed vascular cambium ring as viewed in a cross-section (i-ii). the vascular cambium ring is completely closed (ii), which later produces secondary xylem (wood) and secondary phloem (iii-iv). In herbaceous plants, secondary growth is limited, meaning that lignification in the cells outside the xylem tissue (dark purple fiber caps on top of the vascular bundles) is essential to strengthening the stems (iii).

## *Exploring xylem anatomy*

Xylem is a complex tissue comprising various cell types, including water-conducting tracheary elements, non-tracheary elements, and parenchyma cells (Evert, 2006; Pittermann, 2010; Słupianek *et al.*, 2021). Tracheary elements, including water-conducting vessel elements and tracheids, are essential components of the xylem tissue. Vessel elements are dead, tubular cells with two large, perforated openings in their lower and upper walls that connect to each other and form an axial row of vessel elements, known as vessels. Vessels typically occur in angiosperms and are, on average, between 1-50 cm long and relatively wide (up to 0.8 mm). Tracheids are mainly present in gymnosperms and are relatively narrow and much shorter and narrower than vessels (ranging from 0.5-4 mm in length and 8-80 µm in diameter; Pittermann, 2010). During development, both types of tracheary elements undergo programmed cell death, resulting in hollow, tube-like cells with lignified secondary walls, which impart mechanical strength to the xylem and allow efficient water transport while preventing cell collapse when xylem sap is under negative pressure (Evert, 2006; Pittermann, 2010; Słupianek *et al.*, 2021). Importantly, both vessels and tracheids are connected laterally and longitudinally via interconduit pits, forming a 3D network of short hollow tubes enabling an efficient long-distance water transport system from roots to leaves (Esau, 1965; Evert, 2006).

Interconduit pits are crucial structures for effective water transport because water needs to pass through millions of these pits in tall trees in order to reach the leaves, simply because the length of tracheary elements is much shorter than the total plant height. Each interconduit pit comprises pit borders, sections of the secondary cell wall that arch over a small aperture and widen into a larger pit chamber. These tiny gaps in the secondary cell wall allow water flow between neighbouring conduits. The intervessel pit membrane, which lies at the center of the pit-pair, is formed by hydrolysis of the middle lamella and primary walls of the two adjacent conduits. In angiosperms, the thickness of the intervessel pit membrane ranges from 70-1200 nm (Meyra *et al.*, 2007; Jansen *et al.*, 2009), and consists of modified porous structures, including microlayers of tightly woven cellulose microfibrils and hemicelluloses, which form a tortuous path of nanoscale pores. The highly interconnected pit membrane pores contain multiple constrictions, with the narrowest constriction in each pore regulating the flow of water, gas, and embolism spreading (Kaack *et al.*, 2019, 2021; Zhang *et al.*, 2020). Pit membranes can account for more than 50% of the total hydraulic resistance in the xylem and are important safety valves that can prevent the spread of embolisms between adjacent conduits, also known as air-seeding, highlighting their crucial role in maintaining the safety and efficiency of the hydraulic system in the xylem network (Sperry *et al.*, 2005; Wheeler *et al.*, 2005; Choat *et al.*, 2006, 2008; Jansen *et al.*, 2009).

Other cell types in angiosperm xylem are fibers, which often comprise the bulk of the xylem tissue, also undergo programmed cell death, and in many cases, surround the vessels. These non-tracheary elements have a short length and often thick lignified walls, which provide the required mechanical support (Jacobsen *et al.*, 2005; Déjardin *et al.*, 2010; Pittermann, 2010). In addition to the dead xylem fibers, angiosperm wood also shows two types of living parenchyma cells, axial parenchyma and ray cells forming radial rays, which remain metabolically active in mature sapwood and contribute to a range of functions, such as the transport of nonstructural carbohydrates and mineral inclusions (O'Brien *et al.*, 2014; Plavcová and Jansen, 2015), water storage (capacitance), xylem hydraulic conductance (Pfautsch *et al.*, 2015), and to a lesser extent, mechanical support (Reiterer *et al.*, 2002; Martínez-Cabrera *et al.*, 2009). Overall, the coordinated actions of these cell types are essential for the proper functioning of xylem tissue in plants.

## *Ascent of sap*

Plants require a continuous water supply between the soil and the leaves in order to sustain essential processes such as photosynthesis, growth, and reproduction (Sperry, 2003; Brodribb, 2009; Lucas *et al.*, 2013; Choat *et al.*, 2018; Brodribb *et al.*, 2020). According to the cohesion-tension theory, water is transported throughout the plant by water-conducting cells (tracheids and/or vessels depending on the plant group), which ensure a chain of interconnected water molecules (Dixon and Joly, 1895; Tyree and Zimmermann, 2002). This theory implies that (1) the root-to-leaf water flow is driven by a gradient of negative pressure (aka tension) that is created in the cell walls of the mesophyll cells in leaves during transpiration, and (2) cohesion forces among water molecules, which are maintained by hydrogen bonds, allow the xylem sap to remain intact under these negative pressures (Dixon and Joly, 1895; Pickard, 1981; Brown, 2013*a*). If the loss of water molecules is larger than the uptake of soil water via the roots, the tension in the xylem sap will increase (Konrad *et al.*, 2019). This negative pressure puts water in a metastable state, which triggers its conversion from the liquid to the vapour phase (i.e., cavitation), which may or may not lead to large gas bubble events (i.e., embolisms) that block the water transport inside the water-conducting cell (Steudle, 2001; Wheeler and Stroock, 2008; Brown, 2013*a*; Venturas *et al.*, 2017) (Figure 3).

Mechanisms involved in embolism formation are complex and poorly known, and involve interactions at the nano-scale inside xylem sap that includes not only water but also other compounds such as tiny (undissolved) gas bubbles, ions, proteins, sugars, and lipids that act as surface active agents (surfactants) (Lens *et al.*, 2022). Cavitation could happen via homogeneous nucleation when water molecules acquire sufficient energy to break intermolecular binding forces, resulting in the formation of an embryonic vapour bubble within the water column. However, this homogeneous nucleation is unlikely to occur since the tension in the xylem conduits is not high enough to allow the cohesion forces to break (Briggs, 1950; Pickard, 1981; Maris and Balibar, 2000; Chen *et al.*, 2016*a*; Kanduč *et al.*, 2020). One alternative hypothesis is that embolism is caused by pre-existing, tiny gas bubbles inside the xylem sap that expand due to various changes in temperature, pressure, surface tension, or gas oversaturation. These changes could trigger a tiny gas nanobubble, surrounded by a stabilizing sheath of surfactants, to expand beyond a critical size that leads to an embolism (Tyree *et al.*, 1994; Schenk *et al.*, 2015, 2017; Ingram *et al.*, 2021). Another alternative is that embolisms are induced by surface bubbles associated with hydrophobic vessel surfaces (Tyree *et al.*, 1994; Lohse and Zhang, 2015).

There is a consensus that the spread of air bubbles via the intervessel pit membranes among adjacent conduits (i.e., air-seeding) is more plausible than the formation of new embolisms in the xylem sap (Zimmermann, 1983; Kaack *et al.*, 2019; Guan *et al.*, 2021). In angiosperms, air-seeding occurs when the xylem sap pressure surpasses the threshold that intervessel pit membranes can sustain, enabling air bubbles in an embolized vessel to be pulled into an adjacent, water-filled vessel through nanoscale pores in pit membranes (Pockman *et al.*, 1995; Sperry and Hacke, 2004; Choat *et al.*, 2008; Jansen *et al.*, 2009). Under drought conditions, low water availability in drying soil or high evaporative demand significantly increases the xylem tension, thereby increasing the risk of air-seeding between adjacent conduits and potentially leading to a cascade effect of more drought-induced embolism as drought progresses (Brodribb and Hill, 2000). If water stress persists, the spread of embolisms in the 3D vessel network continues to decrease hydraulic conductivity and could eventually lead to decreased photosynthesis, desiccation, dieback of tissues and organs, and, ultimately, plant mortality (Brodribb and Cochard, 2009; Urli *et al.*, 2013; Adams *et al.*, 2017; Mantova *et al.*, 2022*a,b*). Bearing this in mind, increasing evidence suggests that natural selection has shaped the hydraulic systems of plants in such a way that the impact of drought-induced embolism is minimized, meaning that plants do not suffer from major drought-induced embolism events in the field under daily, natural growing conditions (Cochard and Delzon, 2013; Delzon and Cochard, 2014; Martin-StPaul *et al.*, 2017; Creek *et al.*, 2020).

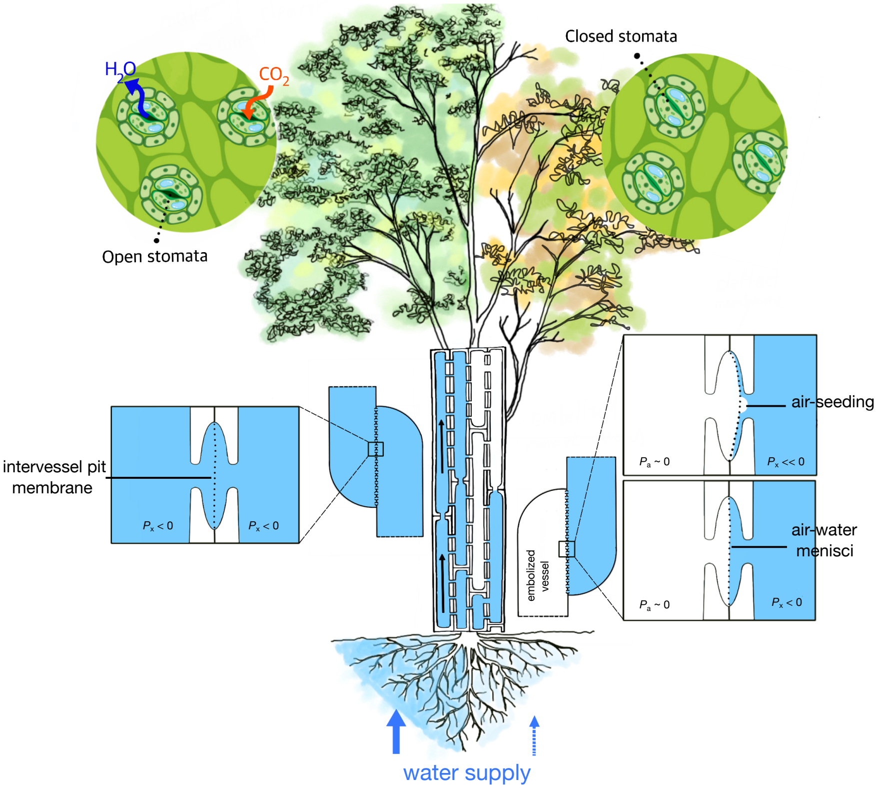

**Figure 3** The root-to-leaf water transport under well-watered (left) and water deficiency conditions (right). In the well-watered stage, water movement is driven by transpiration occurring through the open stomata during the day. As water evaporates from the leaves, it creates a negative pressure that draws water up from the roots, creating a continuous flow of water through the plant. During the onset of drought, the stomata close in an effort to prevent water loss and subsequently a continuously declining negative xylem sap pressure as this would otherwise promote embolism spread via air-seeding (visualized as a simplified 2D cartoon on the right-hand side). Air seeding thresholds in angiosperms are set by the thickness of the intervessel pit membrane, its associate pit membrane pore size, and the number of intervessel pits for a given conduit of average size. *Adapted from Venturas et al. (2017).*

## *Assessing plant vulnerability to embolism*

The vulnerability of plants to embolism can be measured by so-called vulnerability curves (VCs), in which the percentage loss of (measured or theoretical) hydraulic conductivity (PLC) is plotted against xylem sap pressure (measured in MPa) (Figure 4A) (Tyree and Sperry, 1989; Choat *et al.*, 2012). The VCs allow us to determine coefficients that have physiological relevance when describing the susceptibility of plants to xylem embolism, facilitating comparisons among plant organs and species (Tyree and Ewers, 1991; Tyree and Zimmermann, 2002). The xylem water potential inducing 50% loss of maximum conductivity ($P_{50}$) is the main parameter derived from VCs. It is a proxy for a plant's drought tolerance (Tyree and Ewers, 1991; Maherali *et al.*, 2004; Choat *et al.*, 2012; Venturas *et al.*, 2017; Brodribb, 2017) (Figure 4A). $P_{50}$ is strongly correlated with water availability reflected by species' distribution patterns and is considered relevant for drought-induced forest mortality modelling (Blackman *et al.*, 2012; Anderegg *et al.*, 2016; Larter *et al.*, 2017; Trueba *et al.*, 2017). Other parameters, such as $P_{12}$ (xylem pressure causing a 12% loss of maximum conductivity) and $P_{88}$ (xylem water potential inducing 88% loss of maximum conductivity), are also used to quantify embolism thresholds (Figure 4A). $P_{12}$ can be interpreted as the 'air entry point', whereas $P_{88}$ is thought to be the lethal threshold for irrecoverable embolism (Brodribb and Cochard, 2009; Meinzer *et al.*, 2009; Urli *et al.*, 2013; Li *et al.*, 2015; Dayer *et al.*, 2020). However, the $P_{88}$ mortality thresholds may not be precise enough, as recent studies indicate that trees were able to recover from water stress beyond $P_{80}$ in conifers or even higher levels of embolism in angiosperms (Hammond *et al.*, 2019; Johnson *et al.*, 2021; Mantova *et al.*, 2021, 2022*b*). Another cavitation index is sensitivity (S), which is represented by the slope of VC. Species with shallow slopes gradually lose hydraulic conductivity over a wide range of xylem pressure. In contrast, the ones with steep slopes experience more rapid cavitation during a small range of $P$ values (Sperry, 1995).

Several mathematical models, such as the Weibull, Gompertz, polynomial functions, and the exponential-sigmoid function, have been used to fit vulnerability curves. Among these, the exponential-sigmoid function is the most widely used model since its parameters represent both susceptibility ($P_{50}$) and sensitivity ($S$) (Rawlings and Cure, 1985; Neufeld *et al.*, 1992; Pammenter and Van der Willigen, 1998; Pockman and Sperry, 2000; Jacobsen *et al.*, 2007*c*). The vulnerability curves can be described as having two general shapes: (1) a sigmoid (s-shaped) curve, and (2) an exponential (r-shaped) curve (Figure 4B). There is increasing evidence that r-shaped curves are due to artefacts (Cochard *et al.*, 2010; Delzon and Cochard, 2014; Martin-StPaul *et al.*, 2014; Torres-Ruiz *et al.*, 2014). The so-called 'open vessel' artefact is the most important one and occurs when vessels are longer than the sample segments, causing multiple vessels to be cut at both ends. This leads to overestimating the vulnerability curve due to the air being sucked into these open vessels during the measurements, resulting in a rapid drop in the percentage loss of conductivity (PLC) at moderate xylem tension (Choat *et al.*, 2010; Cochard *et al.*, 2010; Wang *et al.*, 2014). However, some authors believe that exponential curves are legitimate and do not result from measurement artefacts (Jacobsen and Pratt, 2012; Sperry *et al.*, 2012; Tobin *et al.*, 2012; Hacke *et al.*, 2014).

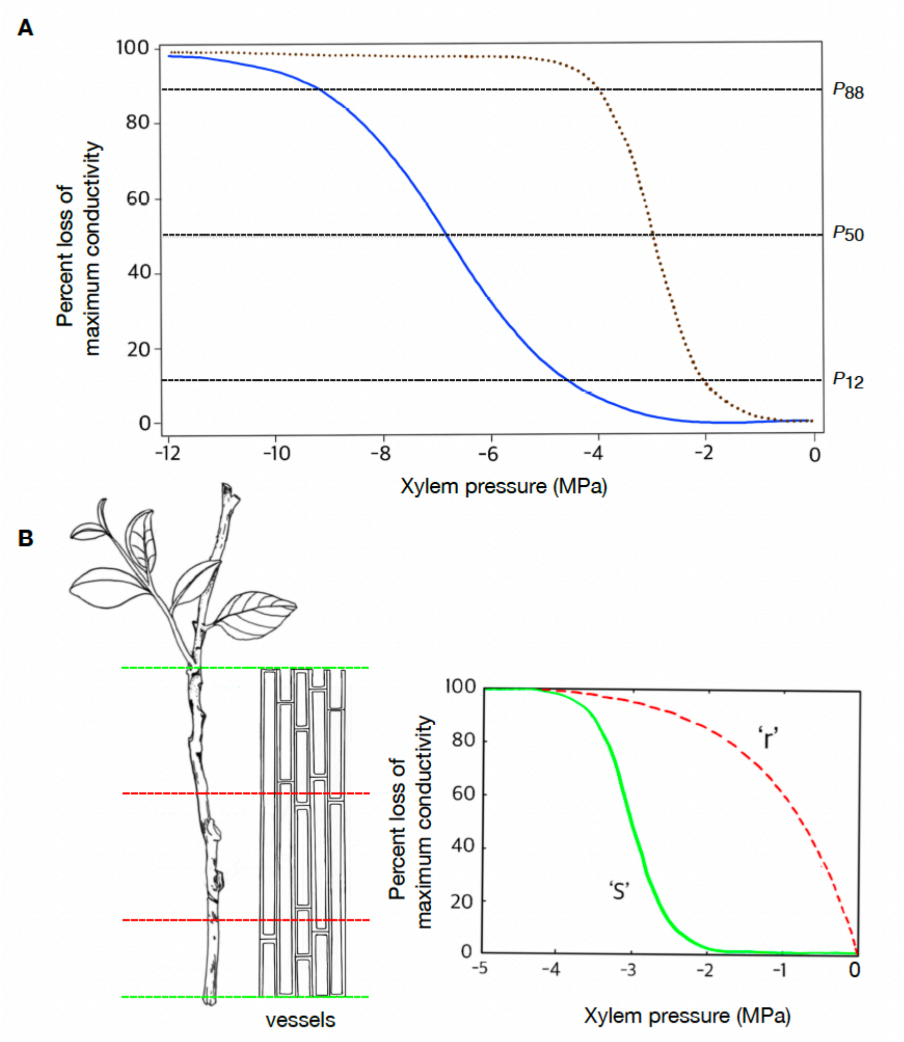

**Figure 4** The xylem vulnerability curve (VC) represents the relationship between the loss of maximum conductivity and xylem pressure. A) The VCs of drought-resistant (blue line) and sensitive species (brown-dotted line) show that a more tolerant plant has more negative $P_{50}$ than a sensitive one, meaning it can withstand better drought-induced embolism inside the xylem. B) The VC is shown as a sigmoidal (green line) and exponential (red-dotted line) curve, demonstrating two different conductivity decline patterns. The r-shaped curve is often attributed to the 'open vessel artefact', which occurs when the stem segment is shorter than the maximum vessel length. These cut-open vessels can be embolized quickly, resulting in a rapid decrease in hydraulic conductivity.

## *Various techniques to build vulnerability curves*

Various experimental methods have been developed to measure the hydraulic conductivity in different organs, ranging from basic approaches to more complex techniques that require special equipment. These techniques vary in the way embolism is induced and quantified (Cochard, 2006; Cochard *et al.*, 2013; Venturas *et al.*, 2017). The four invasive (i.e., requirement of cutting) approaches used to construct vulnerability curves are (1) bench dehydration, (2) air injection, (3) the centrifuge-based method, and (4) the pneumatic method, which are described below.

*(1)* *Bench dehydration* is a basic procedure that best resembles actual drought-stress dehydration in plants (Figure 5A). With this technique, embolism is evaluated after whole intact plants (in situ or potted) or large excised segments (e.g., branches > 1 m long) are dehydrated freely in the air, expressing a range of different xylem pressures. During the drying process, leaf water potential is measured from a drying plant, and a stem segment close to the measured leaf is taken and plugged into water-filled tubes allowing to measure the amount of water flow through the stem segment at a given leaf water potential value. Bench dehydration is a time-consuming process, as dehydration of the samples might take days to weeks. In addition, several plant segments are required to construct one VC (Sperry and Tyree, 1988; Tyree *et al.*, 1992; Bréda *et al.*, 1993; Cochard *et al.*, 2013). This technique is preferred for long-vessel species (e.g., ring-porous trees and lianas) and was long considered as the golden standard to make VCs (Choat *et al.*, 2010).

*(2)* The *air injection* method uses positive gas pressure to induce embolism in shorter sample segments (stems or roots) (Sperry and Tyree, 1988). Cavitation is induced by increasing the air pressure inside the chamber that holds the stem or root segment. The air can be injected into the segments when only one side is cut (single-end air injection) or through the segment surface in a double-ended pressure chamber with the two cut ends of the sample protruding out of the chamber (Cochard *et al.*, 1992; Salleo *et al.*, 1992; Sperry and Saliendra, 1994; Ennajeh *et al.*, 2011). Embolism is subsequently measured by measuring the water flow through the stems-roots at

different levels of positive pressure until the water flow drops to nearly zero (Figure 5B). The main advantage of this technique is that water flow can be controlled with great accuracy and applied to the sample within minutes (Ennajeh *et al.*, 2011; Cochard *et al.*, 2013), but is also prone to open vessel artefact (Cochard *et al.*, 2013).

*(3)* The *centrifuge-based method* uses centrifugal force to generate a specific negative pressure in the middle part of the stem or root segment, after which the water flow in the segments is repeatedly measured at each centrifugation-induced pressure step (Pockman *et al.*, 1995; Alder *et al.*, 1997; Cochard, 2002; Cochard *et al.*, 2005, 2010) (Figure 5C). The centrifugation technique, as well as air injection, enables the construction of a whole VC on one sample, thus reducing sample variability (Cochard *et al.*, 2013; Martin-StPaul *et al.*, 2014; Venturas *et al.*, 2017). An additional advantage of the centrifugation technique is that it can also be applied to stems of small herbaceous species, such as Arabidopsis, which cannot be done with an air injection method (Tixier *et al.*, 2013).

*(4)* The *pneumatic method* estimates xylem vulnerability for a single branch by extracting gas from xylem tissues through a partial vacuum applied to a cut segment (stem, petiole, or root) under various water potentials (Figure 5D). The advantage of this approach is that the pneumatic device is an easy, low-cost, and powerful tool for field measurements (Pereira *et al.*, 2016, 2020).

Despite numerous consistent results produced using these invasive methods, methodological debates have been raised over the years due to various potential artefacts that appear when investigating a system that is under negative pressure. Indeed, techniques that rely on cutting samples potentially allow air and other impurities to enter the segment, resulting in biased results (Wheeler *et al.*, 2013; Cochard *et al.*, 2013; Rockwell *et al.*, 2014; Martin-StPaul *et al.*, 2014; Wang *et al.*, 2014; Venturas *et al.*, 2017). One of the most influential artefacts is the open vessel artefact that regularly occurs when measuring angiosperm species with the popular centrifugation or air injection technique (Choat *et al.*, 2010; Cochard *et al.*, 2010; Martin-StPaul *et al.*, 2014; Torres-Ruiz *et al.*, 2014; Torres-Ruiz *et al.*, 2017). Therefore, in order to detect embolisms in a non-destructive manner, non-invasive imaging approaches have been developed. High-resolution X-ray computed tomography (HRCT) is an imaging method that uses a high-intensity X-ray source with a micrometer-range resolution to detect whether a conduit is water-filled or air-filled (light grey or dark as viewed in virtual microCT images, respectively). The development of HRCT has made it possible to visualize the three-dimensional structure of the vessel network and simulate how embolisms propagate through the xylem network when the plant is subjected to drought (Brodersen *et al.*, 2010, 2011) (Figure 5E). Another non-invasive technique that visualizes the spatial, temporal spread of embolisms in the leaf venation network during water stress is the optical vulnerability (OV) approach (Figure 5F). By recording and comparing changes in the transmission of light through the veins of leaf samples, the OV method detects and follows the spread of embolisms as drought progresses (Brodribb *et al.*, 2016*b*). Moreover, this method also allows for measuring embolism resistance in stems, roots as well as flowers (and leaves) of the same individual (Zhang and Brodribb, 2017; Rodriguez-Dominguez *et al.*, 2018; Bourbia *et al.*, 2020; Song *et al.*, 2022), enabling to compare embolism resistance of different organs within the same individual. In addition to HRCT and OV, the acoustic emission method (AE) can be used as a non-invasive, real-time monitoring tool for assessing drought-induced embolism in plants. AE indirectly measures the loss of hydraulic conductivity by placing sensitive acoustic sensors, such as piezoelectric transducers, onto plant stems (with or without bark) or leaves (Figure 5G). These sensors can capture ultrasonic frequency ranges, including those emitted during cavitation events (100-200 kHz). Despite the practical advantages of this method, being automatic and less labour intensive compared to other techniques, AE requires precise setup and calibration of the sensors, which demands special expertise. Another challenge lies in effectively distinguishing the embolism-related AE signals from the signals caused by other processes, which is necessary to conduct precise data analyses and accurate interpretation (Vergeynst *et al.*, 2015*a*,*b*, 2016; De Roo *et al.*, 2016; Oletić *et al.*, 2023).

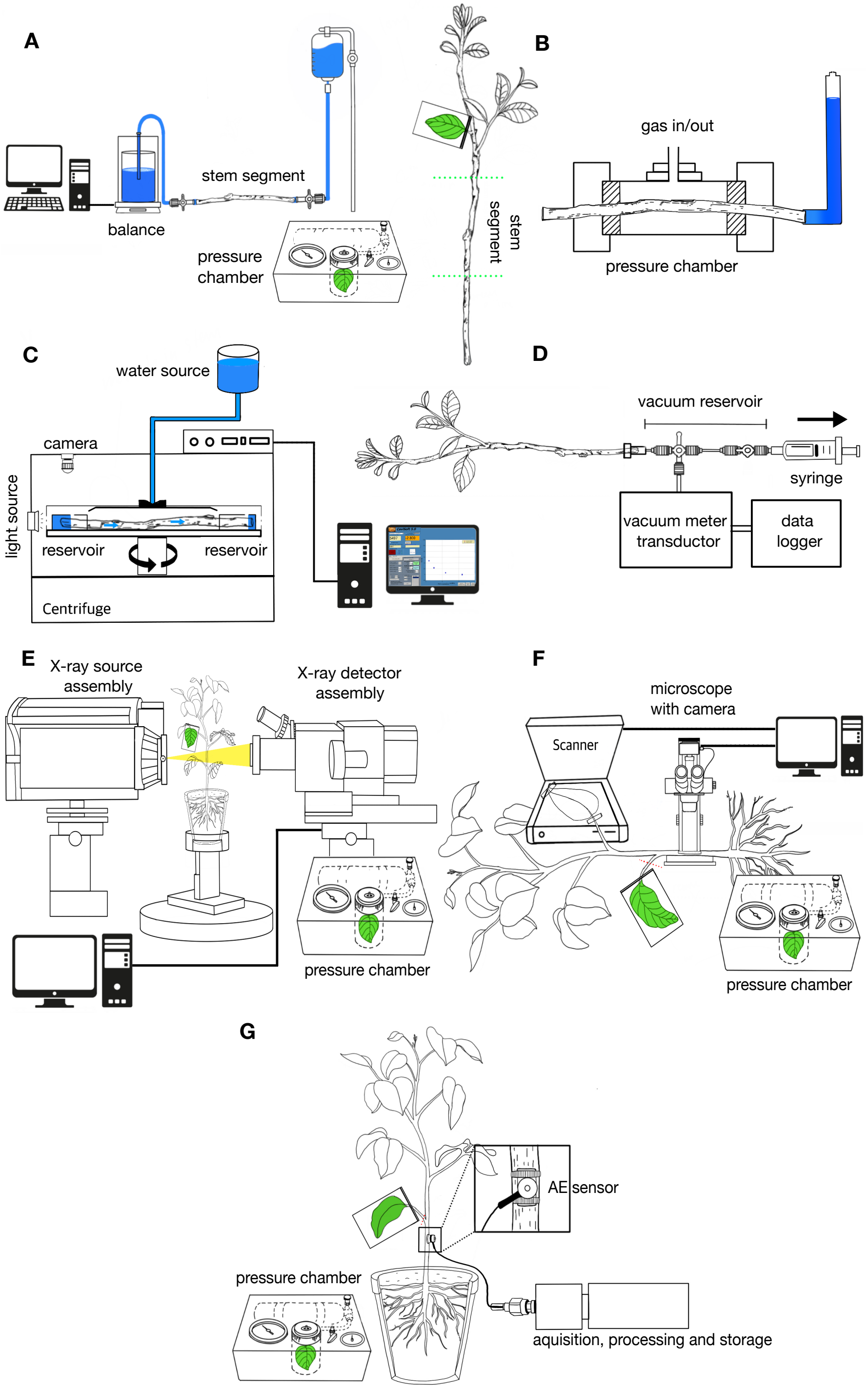
A
stem segment
balance
pressure chamber
B
stem segment
gas in/out
pressure chamber
C
water source
camera
light source
reservoir
reservoir
Centrifuge
D
vacuum reservoir
syringe
vacuum meter transductor
data logger
E
X-ray source assembly
X-ray detector assembly
pressure chamber
F
microscope with camera
Scanner
pressure chamber
G
AE sensor
pressure chamber
aquisition, processing and storage

**Figure 5** The diagram illustrating different techniques used for measuring vulnerability curves (VCs). A) Bench dehydration technique measuring water transport in a freshly excised stem from a larger branch that is drying out in the lab; for each excised stem, the leaf water potential is measured until the water flow reduces to nearly zero in the last stem segment from the branch; *based on Sperry and Tyree (1988)*. B) Air injection method in double-end pressure chamber used for measuring the water flow through the stems-roots at different levels of positive pressure until the water flow drops to nearly zero*; adapted from Cochard et al. (1992) and Ennajeh et al. (2011)*. C) Custom-built cavitron centrifugation measuring water flow through the excised stem segment while simultaneously creating more negative xylem pressures by spinning the stems with increasing rotation speed steps; *adapted from Cochard et al. (2002, 2005)*. D) Pneumatic method is shown in the measurement position. The vacuum is created with a syringe directly connected to the tube, and the stopcocks are closed to the vacuum reservoir and open to the branch and vacuum meter. By pulling the syringe, the vacuum is created. Thereby the gas is sucked from the stem. The amount of gas/air discharged (AD) from the sample is measured over time while the plant tissue desiccates until AD reaches a plateau (stops increasing); *adapted from Pereira et al. (2016)*. E) High-resolution X-ray computed tomography (HRCT) makes virtual stem sections of living plants that are put under drought stress. These virtual sections can be used to visualize whether conduits are water-filled or gas-filled, and dynamics of embolism can be followed when plants are drying out more. Based on the proportion of the conduit area of all water-filled vessels compared to the total vessel area, and the leaf water potential at different time points, a VC can be made; *adapted from Brodersen et al. (2010)*. F) Optical vulnerability technique with scanner and microscope measuring intact plants that are put under drought stress. Every 5 minutes, images are taken from a leaf (with a scanner) and the stem (with a stereomicroscope equipped with a digital camera) from the same individual simultaneously. Subsequent images of the leaf and stem are analyzed, looking for differences in pixels that resemble the sudden change from water-filled to embolized conduits until nearly all conduits are embolized*; adapted from Brodribb et al. (2016)*. G) The acoustic emission (AE) method employs a transducer attached to the plant stem, which consistently captures AE signals emitted by the plant under drought stress conditions. The integrated AE sensor system runs signal acquisition, signal feature extraction, and results are logged onto a SD card; *adapted from Oletić et al. (2023)*.

## *Surviving and thriving: how plants respond to drought*

Plant mortality is intimately linked to the balance between water supply and demand. However, carbohydrate availability also plays a role in the hydraulic function and associated failure, making both water and carbon supply crucial for plant survival (Allen *et al.*, 2015; Martinez-Vilalta *et al.*, 2019; Kannenberg *et al.*, 2021). To cope with water-deficit conditions, plants have evolved a range of strategies, including several functional traits in different organs that minimize the effects of drought stress and maximize their performance and fitness (Violle *et al.*, 2007). Resistance to drought-induced embolism can vary within and across species in response to various environmental factors such as water availability and shade (Stiller, 2009; Plavcová *et al.*, 2011). This resistance can be achieved by, among others, building the xylem resistance (Larter *et al.*, 2017), preventing sap pressure from reaching critical thresholds through early closure of the stomata (Martin-StPaul *et al.*, 2017), or contributing to hydraulic recovery by developing new wood tissue (Gauthey *et al.*, 2022). The coordination of drought-related features within and among organs is crucial in determining how long plants can maintain metabolic activities without risking hydraulic failure. For example, some plants may develop deep roots or other root-related traits that improve water uptake, while others may have leaf characteristics that limit water loss through transpiration (Allen *et al.*, 2009; Choat *et al.*, 2012; Mitchell *et al.*, 2013; Martínez-Vilalta and Garcia-Forner, 2017; Buckley, 2019; Creek *et al.*, 2020; Limousin *et al.*, 2022). By combining these traits, plants can optimize their water use efficiency and improve their chances of surviving periods of water shortage. Ultimately, understanding the mechanisms underlying plant responses to drought stress by investigating the diversity of drought-associated plant traits is essential for developing strategies to improve plant resilience and productivity in water-limited environments (Choat *et al.*, 2012, 2018; Blackman *et al.*, 2019; Rosas *et al.*, 2019; Venturas *et al.*, 2021; Lens *et al.*, 2022).

## *Stomatal regulation*

Stomata are microscopic structures found on the surface of leaves. They regulate the exchange of gases, mainly carbon dioxide ($CO_2$) and oxygen ($O_2$), between plants and the atmosphere and the loss of water vapour by transpiration (Lawson and Vialet-Chabrand, 2019). Stomata are pores surrounded by a pair of guard cells whose size can be altered in response to environmental signals, thereby regulating the rate of gas and water exchange (Wall *et al.*, 2022). This ability to adjust stomatal conductance ($g_s$) is an essential adaptive feature that enables plants to maintain a balance of water use efficiency (WUE, defined as the ratio of photosynthesis and transpiration), especially under changing environmental conditions such as vapour pressure deficit (VPD), temperature, light levels, atmospheric $CO_2$, and soil water availability (Assmann and Wang, 2001; Buckley, 2005; Messinger *et al.*, 2006; Ainsworth and Rogers, 2007). The regulation of stomatal opening and closure in response to drought is a complex process involving physical and biochemical changes. When the soil water becomes scarce, the plant senses the change and triggers a series of responses to reduce water loss through transpiration and delay xylem sap pressures from reaching critical thresholds (Brodribb and Holbrook, 2003; Pittermann, 2010; Buckley, 2019). One of the primary responses to drought is the closure of stomata, which considerably reduces the transpiration rate (although there will always be a residual stomatal conductance when the stomata are closed; see Billon *et al.*, 2020). Therefore, water is conserved for important processes, such as maintaining cellular turgor pressure. However, stomatal closure also results in a decline in carbon uptake as photosynthetic rates drop in response to decreased gas exchange (McDowell *et al.*, 2008; Brodribb *et al.*, 2017*b*; Martínez-Vilalta and Garcia-Forner, 2017; Martin-StPaul *et al.*, 2017; Knipfer *et al.*, 2020). As drought progresses, xylem water potential starts to become slightly more negative, leading to a decline in stomatal conductance to near zero. This closure is usually performed before the onset of substantial embolism formation to avoid the possibility of hydraulic failure (Brodribb *et al.*, 2003; Martin-StPaul *et al.*, 2017; Scoffoni *et al.*, 2017; Choat *et al.*, 2018). However, some plants try to keep their stomata open during drought as long as possible to maximize carbon assimilation, especially in species that are extremely resistant to embolism formation (see next paragraph). In other words, plants have evolved a range of stomatal conductance regulation mechanisms to achieve optimal water use efficiency in response to drought. These responses can vary across plant species, depending on their control strategies and physiological traits (Klein, 2014; Buckley, 2019; Papastefanou *et al.*, 2020; Joshi *et al.*, 2022).

Two stomatal regulation behaviors in response to drought stress have been described: isohydric and anisohydric (Bonal and Guehl, 2001;

West *et al.*, 2007; McDowell *et al.*, 2008). Isohydric species or drought avoiders ($P_{50}$ value close to zero) tend to maintain a constant level of leaf water potential, even under severe drought stress, by tightly regulating the stomatal openings. In reaction to periods of water shortage, these plants close their stomata very early, regardless of the potential carbon loss. This strategy permits greater control over the plant's water balance but can come at the cost of diminished photosynthetic rates and growth due to limited gas exchange. Anisohydric plants or drought-tolerant species (much more negative $P_{50}$ value), however, exhibit a more relaxed control over the stomatal aperture. These plants tend to keep their stomata open longer for greater photosynthesis and growth rates under mild drought stress. However, as drought stress intensifies, anisohydric species also ultimately close their stomata to conserve water and to avoid hydraulic failure (McDowell *et al.*, 2008; Klein, 2014; Joshi *et al.*, 2022). Importantly, recent research has demonstrated that isohydric, and anisohydric strategies are not fixed to one extreme side but rather exhibit dynamic responses to changes in water availability (Papastefanou *et al.*, 2020).

## *Stomatal safety margin*

As mentioned above, stomatal regulation is crucial for plants to maintain the water balance and prevent hydraulic failure during drought stress (McDowell *et al.*, 2008; Brodribb *et al.*, 2017*b*; Martínez-Vilalta and Garcia-Forner, 2017; Martin-StPaul *et al.*, 2017; Knipfer *et al.*, 2020). Therefore, measuring $P_{50}$ alone may not accurately reflect plant embolism resistance, as it does not account for the role of stomatal regulation. In addition, $P_{50}$ values are typically considered constant over time by taking only a single point during the season (Lobo *et al.*, 2018; Mauri *et al.*, 2020; Martínez-Vilalta *et al.*, 2021). However, this is not entirely accurate, as research has shown that $P_{50}$ can vary across seasons. For instance, $P_{50}$ values may become more negative at the end of the growing season when conditions are becoming drier and warmer (Kolb and Sperry, 1999; Jacobsen *et al.*, 2007*b*; Charrier *et al.*, 2018; Sorek *et al.*, 2022). Consequently, combining stomatal closure with $P_{50}$ results is a more physiologically relevant approach to estimating the ability of a plant species to withstand drought-induced embolism (Meinzer *et al.*, 2009; Anderegg *et al.*, 2016; Martin-StPaul *et al.*, 2017; Creek *et al.*, 2020; Dayer *et al.*, 2020; Skelton *et al.*, 2021). This is captured in the so-called stomatal safety margin (SSM), defined as the difference between the water potential at stomatal closure ($\Psi_{gs90}$) and the pressure inducing 50% loss of hydraulic conductance ($P_{50}$) (Figure 6). By measuring SSM, it is possible to evaluate the level of native embolism resistance in plants at a given drought period, which will be negligible in species with a wide SSM showing a large buffer between the point of stomatal closure and the point of hydraulic failure (often around or beyond $P_{88}$). In contrast, plants with narrower (or even negative) safety margins operate closer to their hydraulic limit and will therefore develop high levels of native embolism - i.e. will more likely face hydraulic failure - even at relatively mild drought periods (Choat *et al.*, 2012; Anderegg *et al.*, 2016; Martin-StPaul *et al.*, 2017; Eller *et al.*, 2018; Creek *et al.*, 2020; Skelton *et al.*, 2021; Oliveira *et al.*, 2021).

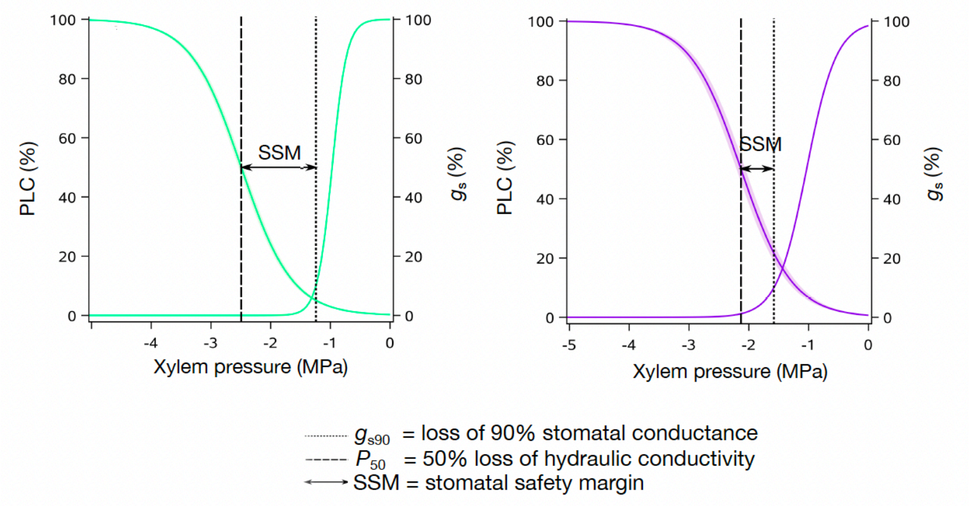

**Figure 6** The graph displaying the stomatal safety margin (SSM), which is the difference between the water potential at near stomatal closure ($\Psi_{gs90}$) and the xylem pressure inducing 50% loss of hydraulic conductance ($P_{50}$). Species with a higher SSM (left) operate further from their hydraulic threshold, either by being more resistant to embolism formation and/or by rapidly closing their stomata during the onset of drought, while species with a low or even negative SSM (right) develop relatively high levels of native embolism even under mild drought stress and will soon reach the critical point of hydraulic failure as the drought intensifies.

## *Ecological trends and trade-offs in xylem anatomy*

In addition to their rapid physiological responses to changes in water availability, plants also have the ability to modify their hydraulic architecture over longer-term responses (Tng *et al.*, 2018). Modifications to the anatomy of xylem tissue are essential for maintaining water transport efficiency and preventing cavitation or embolism under drought stress. The potential roles of different xylem cell types, sizes, and arrangements, as well as their environmental factors, were first explored in studies that compared the wood anatomy of different species growing in contrasting environments, a subdiscipline known as ecological wood anatomy (Carlquist, 1975, 1980; Baas, 1976; Baas *et al.*, 1983; Alves and Angyalossy-Alfonso, 2000; Segala Alves and Angyalossy-Alfonso, 2002; Lens *et al.*, 2004). As a result, numerous ecological trends associated with wood anatomical variation from diverse habitats, varying in water availability, temperature, and elevation, have been suggested. For instance, in drier environments, woody species tend to have narrower vessels with higher density, and thicker fiber walls compared to closely related species thriving in wetter conditions (Carlquist, 1966, 1977; Baas *et al.*, 1983; Carlquist and Hoekman, 1985; Bosio *et al.*, 2010).

Xylem tissue of plants provides two fundamental functions, water transport and mechanical support, which create competing demands. These conflicts can lead to a trade-off between efficiency and safety, meaning that when plants prioritize one function, such as water transport efficiency, they may compromise their ability to provide mechanical support (Tyree and Sperry, 1989; Baas *et al.*, 2004; Hacke *et al.*, 2006; Sperry *et al.*, 2006, 2008; Venturas *et al.*, 2017) (Figure 7). A pervasive hypothesis concerning the trade-off between hydraulic safety and efficiency has been proposed for a very long time (Zimmerman and Brown, 1971). Larger and longer vessels are linked to more efficiency in water conduction than narrower and shorter vessels, allowing plants to photosynthesize more and grow faster under favorable conditions (Poorter *et al.*, 2010; Gleason *et al.*, 2012, 2016*a*; Bouda *et al.*, 2019). However, enhancing embolism resistance, which requires investing more in increasing conduit wall and fiber wall thickness, might impair hydraulic efficiency (Tyree *et al.*, 1994; Hacke *et al.*, 2001, 2006; Jacobsen *et al.*, 2007*b*; Sperry *et al.*, 2008; Meinzer *et al.*, 2010). To achieve a balance between safety and efficiency, plants have developed different strategies depending on their ecological and environmental conditions. Some species value safety over efficiency, while others value efficiency more than safety (Tyree *et al.*, 1994; Hacke *et al.*, 2006; Sperry *et al.*, 2008; Meinzer *et al.*, 2010). Interestingly, there is a substantial number of species that exhibit no trade-off because they have poor performance in both efficiency and safety (Choat *et al.*, 2005; Gleason *et al.*, 2016*b*).

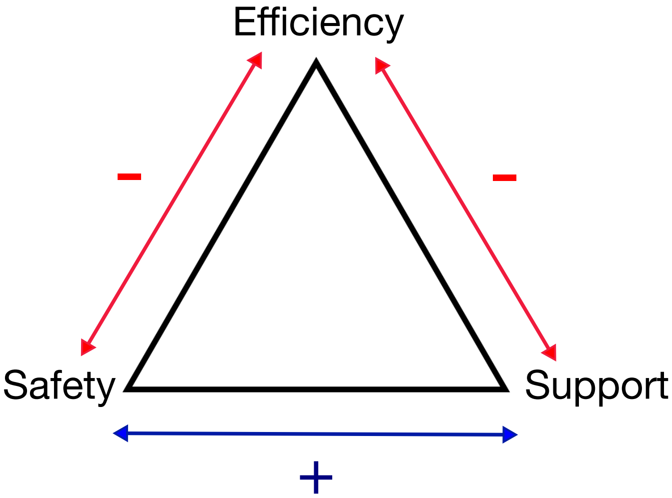

**Figure 7** "Trade-off" triangle showing the relationships amongst xylem functions. Efficiency refers to conductivity efficiency ($K_s$ in $m^2MPa^{-1}s^{-1}$); safety refers to resistance to embolism (MPa), and support refers to mechanical strength (vessel and fiber wall thickness). The conductive efficiency is inversely proportional to both mechanical strength and resistance to embolism. *Adapted from Baas et al., 2004.*

## *Structure-function relationships in the xylem*

A range of wood traits has been found to be associated with resistance to embolism. One such trait is wood density (WD), which is believed to impact water transport because of its correlation with the total area of the conduit area (Pratt *et al.*, 2007*b*; Chave *et al.*, 2009). Increased wood density tends to decrease hydraulic capacity, low water storage capacity and high construction costs (Pratt *et al.*, 2007*a*; Meinzer *et al.*, 2008*a*,*b*; Scholz *et al.*, 2011). Species with high wood density typically resist drought-induced embolism (Hacke *et al.*, 2001; Jacobsen *et al.*, 2007*a*; Willson *et al.*, 2008; Hoffmann *et al.*, 2011), mechanical breakage (Niklas, 1997; Poorter, 2008), and attack by pathogens and fungi (Augspurger and Kelly, 1984). In addition, recent studies have shown convincing physiological evidence that species with dense wood are better able to survive at low water potentials due to their lower leaf/xylem turgor loss point (Fu and Meinzer, 2019; De Guzman *et al.*, 2021). Consequently, tree species with greater wood density tend to have lower mortality rates but are known to grow more slowly (Chao *et al.*, 2008; Nardini *et al.*, 2013; Greenwood *et al.*, 2017). WD is associated with the investment in various anatomical features, including vessel wall thickness and the surrounding fiber matrix that is hypothesized to protect vessels from collapsing during progressive xylem tension (although conduit collapse has only been sporadically observed in leaves) (Hacke *et al.*, 2001; Jacobsen *et al.*, 2005, 2007; Pratt *et al.*, 2007; Russo *et al.*, 2010; Zheng and Martínez-Cabrera, 2013; Fortunel *et al.*, 2014; Dória *et al.*, 2018; Zhang *et al.*, 2023). Plants with a greater degree of embolism resistance are also thought to develop thicker vessel walls relative to their lumen diameter (higher thickness-to-span ratio expressed by (t/b)) (Hacke *et al.*, 2001; Sperry and Hacke, 2004; Jacobsen *et al.*, 2005, 2007*a*; Pittermann *et al.*, 2006). Likewise, the surrounding fiber cells might also contribute to embolism resistance by reinforcing the vessel wall, regardless of changes in vessel wall thickness or lumen diameter (Jacobsen *et al.*, 2005). Thus, greater investment in the vessel and fiber walls results in higher wood density, which reflects the ability of a plant to resist embolism. In herbaceous species, which lack a woody structure, higher stem density results from increased lignification in the stem. In addition, the amount of lignin accumulated in the cell wall could influence the speed of embolism by affecting gas diffusion kinetics across vessel walls, suggesting that stems with higher lignification levels may have a slower rate of embolism propagation (Lens *et al.*, 2016; Pereira *et al.*, 2018; Dória *et al.*, 2018; Lens *et al.*, 2022). Lastly, modifications of lignin concentration and composition in different cell types, such as vessels or fibers, can influence the mechanical and hydraulic properties of the stem. These alterations can boost cell stiffness, flexibility, and hydrophobicity of the cell wall, which can impact the plant's ability to withstand and recover from drought stress (Pereira *et al.*, 2018; Ménard *et al.*, 2022).

Vessel connectivity is another trait that has been linked to drought-induced embolism (Levionnois *et al.*, 2021; Mrad *et al.*, 2021; Ewers *et al.*, 2023). The average vessel connectivity (C) represents the number of neighboring vessels averaged over all vessels in the xylem segment (Loepfe *et al.*, 2007; Martinez-Vilalta *et al.*, 2012). Unfortunately, due to methodological constraints, vessel connectivity has rarely been investigated. Instead, the vessel grouping index ($V_G$) has been widely quantified and used as a 2D proxy of C (Mrad *et al.*, 2021). Some studies have found that high vessel grouping is associated with increased embolism resistance (Lens *et al.*, 2011; Levionnois *et al.*, 2021; Lemaire *et al.*, 2021*b*). This is because it provides a hydraulic redundancy pathway, which reduces the potential loss of water transport capacity associated with the embolism (Carlquist, 1984; Tyree *et al.*, 1994). In other words, connections with adjacent vessels offer alternative routes for water transport when some vessels are embolized (Carlquist, 1984; Tyree *et al.*, 1994; Levionnois *et al.*, 2021). However, some studies suggested that high $V_G$ increases the likelihood of embolism spreading, resulting in a lower hydraulic safety (Loepfe *et al.*, 2007; Martinez-Vilalta *et al.*, 2012; Scholz *et al.*, 2013*b*). Therefore, there is controversy about the impact of the degree of vessel grouping on embolism resistance. Interestingly, Mrad *et al*. (2021), based on wood anatomy in *Acer*, simulated xylem segments and linked vessel connectivity to VC and hydraulic conductivity, suggesting that increasing vessel connectivity and grouping improves the resistance to embolism without compromising hydraulic efficiency. Additionally, the simulation showed that vessel connectivity significantly affects the slope of the VC. Thus, vessel grouping is necessary for the resistance to embolism spread, yet it also needs to be accompanied by variations in pits and other vessel traits (Lemaire *et al.*, 2021*b*; Mrad *et al.*, 2021).

One of the most frequently measured and debated anatomical traits associated with resistance to drought-induced embolism is vessel diameter (D). Comparative and ecological wood anatomy studies have suggested a positive correlation between conduit diameter and embolism resistance. Several arguments have been raised (see Olson *et al.*, 2023 for an overview). Experimental research on xylem vulnerability to drought-induced embolism, however, shows no solid evidence for a direct link between vessel diameter and embolism resistance. For instance, several studies have found that narrow vessels in leaves are more vulnerable to embolism than wider vessels in shoots (Pivovaroff *et al.*, 2014; Charrier *et al.*, 2016; Johnson *et al.*, 2016; Creek *et al.*, 2018; Skelton *et al.*, 2019), which may also suggest a vulnerability segmentation hypothesis (Tyree and Ewers, 1991). This hypothesis assumes that xylem in different plant organs has varying levels of embolism resistance, with more distal tissues, such as leaves and twigs, being more vulnerable than more proximal tissues (Tyree and Ewers, 1991).

However, recent studies have found that the xylem tissue in leaves, stems, and roots has (more or less) the same embolism resistance although the vessel diameter considerable changes among organs (Skelton *et al.*, 2017; Creek *et al.*, 2018; Wason *et al.*, 2018; Losso *et al.*, 2019; Levionnois *et al.*, 2020; Smith-Martin *et al.*, 2020; Lübbe *et al.*, 2022). Other traits that might involve in the mechanisms underlying drought-induced embolism, such as intervessel pit traits, may be better predictors of embolism vulnerability than vessel diameter (Lens *et al.*, 2022).

During the last two decades, it has become increasingly clear that intervessel pit membranes are key structures in the root-to-shoot water transport, which considerably impact the resistance to flow, and function as a safety valve by minimizing the spread of embolism from non-functional vessels to neighbouring functional conduits (Sperry and Tyree, 1988; Tyree and Zimmermann, 2002; Meyra *et al.*, 2007; Choat *et al.*, 2008). This protective function in intervessel pit membranes is enabled by the pit membrane's tiny pore constrictions and high permeability, which enable the flow of gas between adjacent vessels (Wheeler *et al.*, 2005; Jansen *et al.*, 2009). The thickness of the intervessel pit membrane ($T_{PM}$) is strongly associated with the plant's ability to resist the spread of embolism, making it one of the main determinants of embolism resistance in angiosperms (Li *et al.*, 2016). Species with thicker pit membranes are more resistant to drought-induced embolism than those with thinner membranes (Jansen *et al.*, 2009; Lens *et al.*, 2011, 2013; Scholz *et al.*, 2013*b*; Schuldt *et al.*, 2016; Li *et al.*, 2016; Bai *et al.*, 2020; Kaack *et al.*, 2021; Isasa *et al.*, 2023) (Figure 8). The relationship between $T_{PM}$ and $P_{50}$ can be functionally explained by the effect that membrane thickness has on the number, size, and distribution of pore constrictions located in these membranes that are considered as nonwoven porous media (Bai *et al.*, 2020). According to the 3D-nanoscale pit membrane structure, the pores between the microfibril layers of pit membranes are extensively interconnected and contain multiple tiny pore constrictions that operate as the bottlenecks for the fluid transport across the pit membrane pathway (Kaack *et al.*, 2019, 2021; Yang *et al.*, 2020; Zhang *et al.*, 2020). Since the thickness of the pit membranes increases with the length of the multiconstriction path, it may be expected that thicker membranes will have a narrower maximum pore constriction size than thinner membranes. In addition, gas bubble snap-offs, which are assumed to occur spontaneously at the air-water interface in pore constrictions, thereby possibly creating surfactant-coated nanobubbles, tend to increase with an increasing number of pore constrictions (Berg *et al.*, 2013; Schenk *et al.*, 2015; Park *et al.*, 2019; Lens *et al.*, 2022)

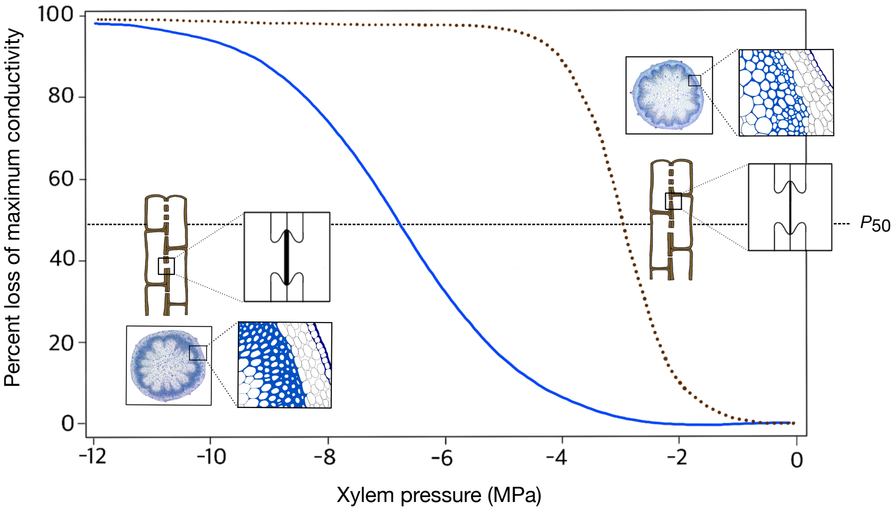

**Figure 8** The xylem vulnerability curve (VC) represents the relationship between the loss of maximum conductivity and xylem pressure. The VCs show that drought-resistant species (more negative $P_{50}$: blue curve) have a woodier or more lignified stem with thicker intervessel pit membranes than the sensitive species (less negative $P_{50}$: brown-dotted curve).

## *Gene networks underlying plant responses to drought stress*

In addition to a multitude of physiological and anatomical traits, plants also respond and adapt to water shortage through molecular mechanisms, which include modifications to the activity of phytohormones, metabolites and signalling pathways, as well as transcriptional regulation cascades (Singh *et al.*, 2022). One of the phytohormones that is well-known for its role in plant acclimatization under stress conditions is abscisic acid (ABA). Under water deficit, ABA is produced, controlling root development, stomata closure, and activating stress-related genes (Nakashima *et al.*, 2014; Förster *et al.*, 2019). After ABA has been accumulated (mainly in leaves), it regulates the expression of downstream drought-inducible genes via *cis*-elements called ABRE (ABA-responsive element) and uses AREB (ABRE binding) genes as major transcriptional activators during ABAmediated signaling (Choi *et al.*, 2000; Uno *et al.*, 2000; Bauerle *et al.*, 2004; Cutler *et al.*, 2010; Maruyama *et al.*, 2012; Mehrotra *et al.*, 2014; Yoshida *et al.*, 2015; Chen *et al.*, 2020) (Figure 9). For instance, in many plant species, *AREB1* overexpression is associated with the improvement of drought resilience (Barbosa *et al.*, 2013; Yoshida *et al.*, 2015; Wang *et al.*, 2016*a*), whereas the triple knockout mutants of *AREB1*, *AREB2* and *ABF3* showed drought stress-sensitive phenotypes and had lower expression of drought-responsive genes (Yoshida *et al.*, 2010). Arabidopsis AREB2 and ABF3 also play a significant role in flowering time regulation by transcriptionally controlling the floral integrator *SUPPRESSOR OF OVEREXPRESSION OF CONSTANS1* (*SOC1*) (Hwang *et al.*, 2019). Under drought stress, elevated ABA levels enhance the activity of *SOC1* through AREB2 and ABF3, thereby accelerating the floral transition and enhancing reproductive success. This adaptive response enables plants to complete their life cycle before the onset of severe drought conditions, thereby mitigating the detrimental effects of water scarcity (Hwang *et al.*, 2019). *SOC1* also emerges as a crucial regulator of various developmental and stress responses (Kimura *et al.*, 2015; Aoki *et al.*, 2019). Moreover, *SOC1*, in conjunction with *FUL* (*FRUITFULL*) and *AHL15* (*AT-HOOK MOTIF CONTAINING NUCLEAR LOCALIZED 15*) (Melzer *et al.*, 2008; Karami *et al.*, 2020; Rahimi *et al.*, 2022) plays a significant role in controlling meristem determinacy and cambial activity. A double loss-of-function mutant of *SOC1* and *FUL* has been shown to suppress axillary meristem maturation, resulting in later-flowering, polycarpic-like woody growth that is characterized by a much longer life span (Melzer et al., 2008). *AHL15* has been found to act downstream of *SOC1* and *FUL*, and enhances vascular cambium activity and hence secondary xylem formation in Arabidopsis inflorescence stems (Rahimi et al., 2022). These woody Arabidopsis genotypes allow us to investigate the role of increased woodiness in the inflorescence stem on the plant's drought response.

In addition to the ABA-dependent system, a number of stress-related genes can be regulated by an ABA-independent regulatory pathway, which is an important process in drought stress response during the initial stages before the build-up of endogenous ABA (Soma *et al.*, 2021)(Figure 9). The important TFs in the ABA-independent system include NAC transcription factors and DRE-binding proteins (DREB), particularly DREB2A (Sakuma *et al.*, 2006*a*,*b*; Lata and Prasad, 2011; Soma *et al.*, 2021). DREB2A, expressed under dehydration and osmotic stress, binds to the Dehydration Responsive Elements (DRE) motif to regulate drought-responsive genes (Maruyama *et al.*, 2012) (Figure 9). Interestingly, the interaction between ABA-dependent and ABA-independent pathways has been observed since several types of TFs control the cellular responses to drought stress. For example, AREB/ABFs can partially regulate the expression of *DREB2A,* showing the interaction between the early processes of drought prior to the accumulation of ABA and the later-occurring ABA-dependent signalling processes (Kim *et al.*, 2011). Furthermore, plant-specific NAC TFs that bind to NAC recognition sites (NACR) mediate environmental stress responses (Tran *et al.*, 2004; Takasaki *et al.*, 2010; Puranik *et al.*, 2012) (Figure 9). For instance, ANAC096 is a positive regulator activated in response to dehydration stress. It increases the expression of drought-responsive genes, specifically *Responsive to Dehydration 29A (RD29A),* which is one of the important marker genes in ABA dependent drought stress signalling pathway (Xu *et al.*, 2013). In conclusion, both ABA-independent and ABA-dependent gene regulatory networks are essential molecular mechanisms that govern differential gene expression during early and later drought responses (Shinozaki *et al.*, 2003; Yamaguchi-Shinozaki and Shinozaki, 2005; Shinozaki and Yamaguchi-Shinozaki, 2006).

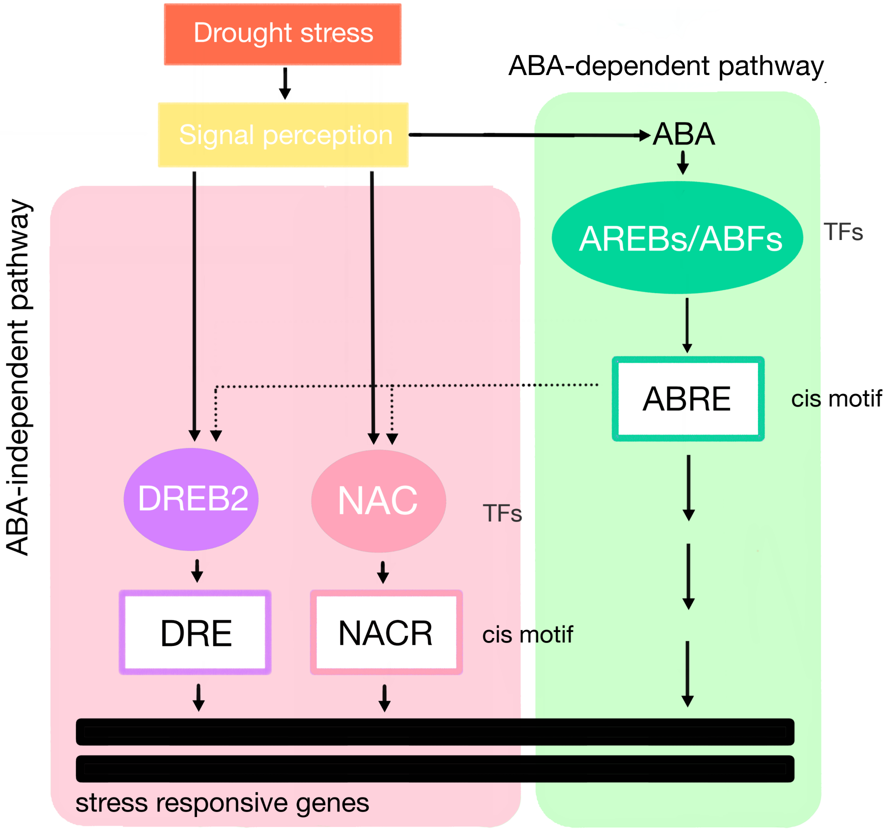

**Figure 9** A schematic model of plant signal perception and regulatory networks under drought stress via ABA-dependent and ABA-independent pathways. ABA signalling, phosphorylate AREB/ABF transcription factors, which in turn induce the expression of stress-responsive genes via an ABA-dependent pathway. DREB2 and NAC transcription factors are activated through an ABA-independent pathway. However, some transcription factors from these two groups, including DREB2A and ANAC096, mediate the crosstalk signal between ABA-dependent and ABA-independent systems. *Adapted from Soma et al. (2021)*.

# Thesis outline

The aim of this thesis is to enhance our understanding of the complex mechanisms underlying drought responses in herbaceous species, providing insights into the various strategies that plants use to cope with drought stress. To achieve this, we investigate the relationship and coordination between xylem anatomical and hydraulic traits in stems and leaves and provide a preliminary analysis of the expression of drought-responsive genes. To address these objectives, we study various genotypes that exhibited contrasting levels of embolism resistance and lignification in the stems of *Arabidopsis thaliana*, a model herbaceous plant, and *Solanum lycopersicum* (tomato), an important crop species. This thesis comprises five chapters, with the first chapter serving as a general introduction and overview of the thesis, followed by the research chapters 2-4 that focus on the research specific objectives, and complemented with the last chapter that provides an overall discussion and conclusion of the PhD results.

## Chapter 2

This chapter delves into identifying the key anatomical and ecophysiological traits that best explain the variation in embolism in the inflorescence stems of four *Arabidopsis thaliana* genotypes with contrasting growth forms. Detailed stem anatomical observations serve as the basis for these explorations.

## Chapter 3

Building upon the previous chapter, this one focuses on studying the drought response strategies of the four Arabidopsis genotypes examined in chapter 2 in more detail, with the addition of two additional genotypes. This investigation combines stem anatomical observations, hydraulic measurements in stems and leaves (during well-watered and drought conditions), and gene expression studies in leaves (during well-watered and drought conditions) to gain comprehensive insights into the plants' adaptive responses to drought.

## Chapter 4

This chapter focuses on investigating the mechanisms underlying the increased drought tolerance observed in J*UNGBRUNNEN1* (*JUB1*) overexpression transgenic lines of both Arabidopsis and *Solanum lycopersicum* L. (tomato). This chapter employs detailed stem anatomy observations in combination with hydraulic traits in stems and leaves of Arabidopsis and tomato plants that differed in expression of *JUB1*, within the context of a drought experiment.